References

ALLEGRA, G., FARINA, M., COLOMBO, A., CASAGRANDE-TETTAMANTI, G., ROSSI, U. & NATTA, G. (1967). *J. Chem. Soc. B*, pp. 1028-1033.

BOYSEN, H. & FORST, R. (1986). *Z. Naturforsch. Teil A*, **41**, 553-559.

CHATANI, Y., ANRAKU, H. & TAKI, Y. (1978). *Mol. Cryst. Liq. Cryst.* **48**, 219-231.

COCHRAN, W., CRICK, F. H. C. & VAND, V. (1952). *Acta Cryst.* **5**, 581-586.

COPE, A. F. G. & PARSONAGE, N. G. (1969). *J. Chem. Thermodyn.* **1**, 99-117.

FINKE, H. L., GROSS, M. E., WADDINGTON, G. & HUFFMAN, H. M. (1954). *J. Am. Chem. Soc.* **76**, 333-341.

FORST, R., JAGODZINSKI, H., BOYSEN, H. & FREY, F. (1984). *Acta Cryst.* A**40**, C144.

LAVES, F., NICOLAIDES, N. & PENG, K. C. (1965). *Z. Kristallogr.* **121**, 258-282.

LE BARS-COMBE, M. & LAJZEROWICZ, J. (1984). *J. Phys. C*, **17**, 669-672.

LE BARS-COMBE, M. & LAJZEROWICZ, J. (1987). *Acta Cryst.* B**43**, 386-393.

PARSONAGE, N. G. & PEMBERTON, R. C. (1967). *Trans. Faraday Soc.* **63**, 311-328.

PEMBERTON, R. C. & PARSONAGE, N. G. (1965). *Trans. Faraday Soc.* **61**, 2112-2121.

TEARE, P. W. (1959). *Acta Cryst.* **12**, 294-300.

Acta Cryst. (1987). B**43**, 398-405

Structure Determination of Benzil in its Two Phases

BY M. MORE, G. ODOU AND J. LEFEBVRE

Laboratoire de Dynamique des Cristaux Moléculaires, UA 801, *Université de Lille I*, 59655 *Villeneuve d'Ascq CEDEX, France*

(*Received* 18 *June* 1986; *accepted* 23 *March* 1987)

Abstract

Benzil, $C_{14}H_{10}O_2$, $M_r = 210{\cdot}2$, Mo $K\alpha$, $\lambda = 0{\cdot}7107$ Å. In the high-temperature phase ($T > 83{\cdot}5$ K), trigonal, $P3_121$, $Z = 3$, $F(000) = 330$, $\mu = 0{\cdot}90$ cm^{-1}. At 294 K, $a = 8{\cdot}402(4)$, $c = 13{\cdot}655(9)$ Å, $V = 835(2)$ Å^3, $D_x = 1{\cdot}253$ g cm^{-3}, $R = 0{\cdot}043$ for 390 reflections. At 100 K, $a = 8{\cdot}356(3)$, $c = 13{\cdot}375(6)$ Å, $V = 809(1)$ Å^3, $D_x = 1{\cdot}294$ g cm^{-3}, $R = 0{\cdot}041$ for 443 reflections. In the low-temperature phase ($T = 70$ K), monoclinic, $P2_1$, $Z = 6$, $F(000) = 660$, $a = 14{\cdot}380(7)$, $b = 8{\cdot}373(4)$, $c = 13{\cdot}359(22)$ Å, $\beta = 88{\cdot}82(5)°$, $V = 1608(4)$ Å^3, $D_x = 1{\cdot}302$ g cm^{-3}, $R = 0{\cdot}066$ for 1893 reflections. The resolution of the low-temperature phase ($T = 70$ K) was possible owing to a new low-temperature attachment for the X-ray four-circle diffractometer. Contrary to what has been previously assumed, the transition corresponds to a doubling of the unit cell. A discussion is developed with these new structural results in order to explain published Raman scattering experiments.

Introduction

In the last few years, considerable efforts have been devoted to the study of the crystalline phase transition of benzil $(C_6H_5{-}CO)_2$ which occurs at 83·5 K. The room-temperature structure has rhombohedral symmetry (Brown & Sadanaga, 1965; Solin & Ramdas, 1968). The space group is $P3_121$ (or the enantiomorph $P3_221$). The benzil molecule has a permanent dipole moment (Higashi, 1938) which coincides with the twofold molecular axis. The hexagonal cell contains three molecules related by the 3_1 screw axis and there is no spontaneous polarization in this phase. Optical birefringence appears near 84 K (Esherick & Kohler, 1973), which indicates a lowering of the symmetry. The transition is reversible with an extremely low latent heat and leads to a twinned crystal (Esherick & Kohler, 1973). Calorimetric investigation (Dworkin & Fuchs, 1977) shows a peak in the heat capacity at 84·07 K and the form of the specific-heat anomaly suggests the first-order nature of the transition. Electron nuclear double resonance (ENDOR) spectroscopy (Chan & Heath, 1979) confirms the presence of domains separated by angular deviations of the order of 1·55° at liquid-helium temperature and the disappearance of the 3_1 screw axis in the low-temperature phase. X-ray studies (Odou, More & Warin, 1978) report that symmetry breaking leads to the triclinic space group $P1$ with a fourfold expansion of the primitive unit cell corresponding to the doubling of the parameters along **a** and **b**. Domain arrangement occurs in such a way that the crystal acquires a pseudo-threefold screw axis and macroscopic polarization vanishes. However, Raman scattering experiments (Sapriel, Boudou & Perigaud, 1979) display a soft optical mode of E symmetry in the high-temperature phase which splits into two (A and B) components in the low-temperature phase, consistent with a monoclinic phase without change in the number of molecules of the unit cell. According to the observation of this optical soft mode and theoretical

0108-7681/87/040398-08$01.50

prediction (Aubry & Pick, 1971), transverse acoustic modes undergo a softening (Vacher, Boissier & Sapriel, 1981) when the temperature is lowered to 83·5 K. Infrared experiments (Wyncke, Brehat & Hadni, 1980) confirm the soft E modes. No conclusions are given about the symmetry of the low-temperature phase, while it is shown that the phase transition involves an increase in the number of molecules in the unit cell.

So, the X-ray experiments were apparently in contradiction with the other results. However, the controversy was ended when X-ray data were shown to be compatible with monoclinic symmetry (Toledano, 1979). In fact, the triclinic unit cell corresponds to the primitive asymmetric unit of the C-faced monoclinic cell. As a consequence, one of the three twofold axes of the high-temperature phase is preserved at the transition.

In agreement with the experimental observations, *i.e.* soft optical modes, change of symmetry and breaking of the translational symmetry, a phenomenological model was built (Toledano, 1979). Based on the Landau theory of phase transitions, this model introduces a double order parameter. A first-order parameter related to the centre of the Brillouin zone ($\mathbf{q}=0$) induces the point-symmetry change, while a second-order parameter, coupled to the former, is associated with the zone-boundary M point ($\mathbf{q}_M=\frac{1}{2},\frac{1}{2},0$) and corresponds to the expansion of the primitive cell. As expected by this model, two transverse acoustic modes have been shown to soften near the phase transition (Yoshihara, Wilber, Bernstein & Raich, 1982) while critical fluctuations for the longitudinal acoustic mode governed by the elastic constant C_{11} appear to be correlated with the zone-boundary mode (Yoshihara, Bernstein & Raich, 1982, 1983). New Raman scattering experiments (Moore, Tekippe, Ramdas & Toledano, 1983) and an X-ray diffuse scattering study (Terauchi, Kojima, Sakaue, Tajiri & Maeda, 1982) have confirmed the validity of the model. The first-order nature of the transition is a result of anharmonic coupling between the two order parameters, and it has been emphasized that the 'benzil phase transition is a unique example of a phase transition for which large anharmonicity plays a dominant role' (Yoshihara *et al.*, 1983). Such a high degree of anharmonicity involves large atomic displacements and justifies structural studies through the phase transition.

Moreover, a critical examination of the X-ray structural report (Odou *et al.*, 1978) should make evident experimental difficulties. The three-dimensional structure was determined by Weissenberg diagrams while the temperature was kept constant at $T=74\text{ K}<T_c$. At this temperature, equi-inclination diagrams show a systematic splitting of diffraction spots arising from the domains and a pseudo-threefold apparent symmetry. As the diffraction patterns of the three domains are superimposed with only 0·6° of angular separation, it is very hazardous to locate systematic extinctions in this way. Indeed, it has been found that some spots were not split, whereas others were split into three parts (Odou, 1976). So the authors studied the splitting of the Bragg peaks with a better accuracy using a two-circle diffractometer and a vertical cryostat. This study concerns the equatorial planes $h0l$, $0kl$ and $hk0$ from which, unfortunately, only a small number of peaks has been measured. Then the assertation of the quadrupling of the unit cell is to be confirmed since the model is based on two statements: (i) the breaking of the point-group symmetry and (ii) the fourfold expansion of the unit cell.

The structure of benzil has been solved in the high-temperature phase at room temperature ($T=294$ K) and at 100 K, and in the low-temperature phase at 70 K.

Experimental

We have emphasized above that we need to study the three-dimensional diffraction pattern of benzil. This can be achieved by using a four-circle diffractometer. In order to obtain the structure of the low-temperature phase we have to cool the crystal to a temperature lower than 80 K and probably less if we want to separate the domains. While very-low-temperature attachments are usual for neutron diffractometers, X-ray four-circle diffractometers until now have mainly used nitrogen-gas flow apparatus which work at temperatures higher than 77 K (90 K in practice). A unique study with a low-temperature cryostat has been reported recently in the literature (Samson, Goldish & Dick, 1980). In our experiments we have used a low-temperature attachment recently built in the laboratory and mounted on a four-circle Huber diffractometer. Details of the apparatus will be published in the near future. Working temperatures are in the range 30–300 K with a precision better than 0·5 K. Angular limitations due to the windows are: $-60<\theta<60°$; $-5<\chi<180°$; $-180<\varphi<180°$. The four-circle diffractometer has been automated using a Mink (PDP 11/03 Digital Equipment) computer and original motor interfaces. All the abilities of standard diffractometers have been implemented: peak searching, centring, automatic zero corrections, automatic data collection *etc.* Special treatments were programmed for the weak peaks in order to increase the peak/noise ratio.

A Philips (PW 1730) generator produces the high voltage of the X-ray tube and works at 1·5 kW (50 kV, 30 mA). The wavelength is 0·7107 Å (Mo $K\alpha$) and the incident beam is monochromated with a pyrolitic graphite crystal. A collimator of 0·8 mm in diameter is used on the incident beam. Diffracted photons are measured by a Philips (PW 1390) counting chain and

an NaI scintillation detector. The absorption variation due to the cryostat windows when the ω-angle varies is negligible.

For the structure determination in benzil in the two phases and for various temperatures (room temperature, 100 and 70 K), about 10 000 reflections have been measured during several weeks without particular difficulties.*

Structure of the high-temperature phase

Single crystals were grown by slow evaporation of a saturated solution of benzil in ethyl alcohol and had a prismatic shape; approximate size $0{\cdot}3\times0{\cdot}4\times0{\cdot}5$ mm.

Intensity measurements were made with the automatic X-ray diffractometer described above at room temperature and at 100 K. Lattice parameters were determined from Bragg angles of 25 selected reflections. To avoid too dissymmetric a background, the ω-scan technique was used with $2<\omega<30°$ [$0{\cdot}05<(\sin\omega)/\lambda<0{\cdot}70$ Å^{-1}]. The total scan width for data collection at room temperature varied according to the relation $1{\cdot}0°+0{\cdot}7°\sin\omega$, while, at 100 K, it had the unvarying width of 1·8°. In both cases, the scan speed was $0{\cdot}020°\,s^{-1}$. The background was counted for half the total scan time on each side of the $K\alpha$ position. Three standard reflections (120, 212 and 210) were monitored every hour for the two measurement temperatures; no significant change in their intensity was observed. 3385 reflections were measured at room temperature ($-10\le h, k\le 10$, $-18\le l\le 18$, Friedel reflections measured) corresponding to 390 non-equivalent reflections with $I>3\sigma(I)$. At 100 K, 2272 reflections were collected ($0\le h, k\le 10$, $0\le l\le 18$, Friedel reflections measured) for 443 non-equivalent reflections with $I>3\sigma(I)$. Data were corrected for Lorentz and polarization effects, but no absorption corrections were applied: at room temperature, $\mu R\simeq 0{\cdot}02$. Six reflections with high intensity and low angle were removed because of the possibility of extinction effects.

The unit cell is trigonal with $Z=3$ and the parameters are: $a=8{\cdot}402(4)$, $c=13{\cdot}655(9)$ Å at room temperature; $a=8{\cdot}356(3)$, $c=13{\cdot}375(6)$ Å at 100 K.

The mean linear thermal expansion coefficients are $\alpha_a=28(4)\times10^{-6}$ and $\alpha_c=106(6)\times10^{-6}\,K^{-1}$, in agreement with our previous determination (Odou *et al.*, 1978).

The systematic absence of $00l$ reflections with $l=3n\pm1$ confirms the existence of a threefold screw axis 3_1 or 3_2. For light atoms like C, O and H forming the benzil molecule, X-rays are not able to distinguish between a 3_1 and a 3_2 screw axis. For this reason, it will be assumed in the following that there is a 3_1 screw axis in the space group of the high-temperature phase of benzil. A good convergence was obtained with $P3_121$ in agreement with the previous structure determination (Brown & Sadanaga, 1965). Crystalline twofold axes correspond to molecular twofold axes.

a_i, b_i and c coefficients for analytical approximation of the scattering factors for C, O and H atoms were from *International Tables for X-ray Crystallography* (1974). From the atomic positions of Brown & Sadanaga (1965), refinements were made on F using *SHELX*76 (Sheldrick, 1976) for the room-temperature data collection. Refinement of positional coordinates and isotropic temperature factors for C and O atoms led the residual R factor to fall to 0·146 ($wR=0{\cdot}138$). Anisotropic temperature factors for non-H atoms and H atoms with isotropic temperature factors were introduced and refined. The final R value is 0·043 ($wR=0{\cdot}040$, unit weights, $S=0{\cdot}53$) for 93 parameters. Shifts in atomic parameters in final cycle were $<0{\cdot}1\,\sigma$. A final difference synthesis showed a maximum residual electronic density of $\pm0{\cdot}09$ e Å^{-3}.

The structure refinement at 100 K started from the atomic positions found at room temperature. With the same conditions as the room-temperature refinement, the reliability R factor was 0·041 ($wR=0{\cdot}042$, $S=0{\cdot}47$). The maximum residual electronic density was ±0.20 e Å^{-3}.

Structure of the low-temperature phase

The single crystal was about the same size as that used for the high-temperature phase. The experiment was performed at 70 K. Crossing of the transition results in domains appearing in the low-temperature phase (Odou *et al.*, 1978). Experimental precautions taken because of the existence of domains are explained in the following.

To determine cell parameters, 25 reflections were chosen: these reflections were scanned and the only reflections kept were those perfectly centred and with one peak (no contributions from other domains appear). To be able to distinguish the intensity of the selected domain, data collection was made using the step-scanning method with 2θ fixed [$2<\omega<30°$; $0{\cdot}05<(\sin\omega)/\lambda<0{\cdot}70$ Å^{-1}]. The total scan width was 1·5° with 75 points on each scan. The measurement time was 1 s per point and the scan was repeated no more than six times to a maximum. Counts were added until the maximal count of the scan reached 800. Each reflection profile was plotted on a screen terminal in order to determine if contributions of other domains occurred. If this was the case and when these contributions were sufficiently separated from the contribution of the selected domain, a program written by the authors was able to suppress them (Fig.

* Lists of structure factors, anisotropic thermal parameters and H-atom parameters have been deposited with the British Library Document Supply Centre as Supplementary Publication No. SUP 43840 (24 pp.). Copies may be obtained through The Executive Secretary, International Union of Crystallography, 5 Abbey Square, Chester CH1 2HU, England.

1). When it was not possible to separate contributions of different domains, an equivalent was measured. Three standard reflections were monitored every hour (220, 021 and 003) and no significant change was observed in their intensities. 4875 reflections were measured ($-18 \le h \le 18$; $0 \le k \le 10$; $0 \le l \le 18$) of which 1893 non-equivalent reflections are such that $I > 3\sigma(I)$ and are quasi-certain to correspond to the intensity of the selected domain. Intensities were corrected from Lorentz and polarization effects, but no absorption corrections were applied.

In a previous study (Odou *et al.*, 1978), a triclinic unit cell for benzil in its low-temperature phase was found from Weissenberg diagrams. In fact, this unit cell corresponds to a monoclinic *C*-face-centred cell with 24 molecules per monoclinic cell (Chan & Heath, 1979). The relationship between this cell ($\mathbf{a}'_m$, $\mathbf{b}'_m$, $\mathbf{c}'_m$; the twofold axis is along $\mathbf{b}'_m$) and the pseudo-hexagonal cell ($\mathbf{a}_H$, $\mathbf{b}_H$, $\mathbf{c}_H$) is $\mathbf{a}'_m = 2(\mathbf{a}_H - \mathbf{b}_H)$; $\mathbf{b}'_m = 2(\mathbf{a}_H + \mathbf{b}_H)$; $\mathbf{c}'_m = \mathbf{c}_H$. The multiplicity of this cell is 4 and reflections defined by (h'_m, k'_m, l'_m) are fundamental reflections when $h'_m + k'_m = 4n$ with h'_m and k'_m even.

Data collection was started with this monoclinic *C*-face-centred cell. It appeared, firstly, that the superlattice reflections with h'_m and k'_m odd have either their intensity equal to zero, or are strongly decentred. Only superlattice reflections with h'_m and k'_m even ($h'_m + k'_m = 4n + 2$) have significant intensity and their position well centred on the position calculated from the *UB* matrix for the selected domain. Taking into account these facts, we think that there is a mistake in the previous determination: superlattice reflections with h'_m and k'_m odd belong to another domain. With these conditions, the monoclinic cell ($\mathbf{a}_m$, $\mathbf{b}_m$, $\mathbf{c}_m$) is primitive with multiplicity 2 only. There are six molecules per unit cell and the relationship between lattice parameters of this cell and the pseudo-hexagonal cell becomes $\mathbf{a}_m = \mathbf{a}_H - \mathbf{b}_H$; $\mathbf{b}_m = \mathbf{a}_H + \mathbf{b}_H$; $\mathbf{c}_m = \mathbf{c}_H$.

The measured lattice parameters are $\mathbf{a}_m = 14{\cdot}380(7)$, $\mathbf{b}_m = 8{\cdot}373(4)$, $\mathbf{c}_m = 13{\cdot}359(22)$ Å and $\beta = 88{\cdot}82(5)°$.

Domains come from the choice of the twofold axis kept in the low-temperature phase, so that there are three possibilities for domains. In Fig. 2, the reciprocal plane perpendicular to $\mathbf{c}^*$ is drawn, with the reciprocal cells of the three domains (the small deformation occurring when the transition is crossed is neglected). As observed experimentally, Fig. 2 shows there is only one intensity contribution for superlattice reflections but a contribution of all domains occurs for fundamental reflections.

Systematic absence of $0k0$ reflections with k odd allows the unambiguous conclusion that the space group is $P2_1$ for benzil in its low-temperature phase. Fig. 3 shows the respective positions of the unit cell of the high- and low-temperature phases perpendicular to the **c** axis.

For the three independent molecules of the unit cell, the starting positional parameters come from those obtained at 100 K using the convenient transformation. In the first cycles of refinement, only C and O atoms were introduced with isotropic temperature factors. It appears, rapidly, that reflections like $\bar{h}hl$ have systematically measured intensities about twice

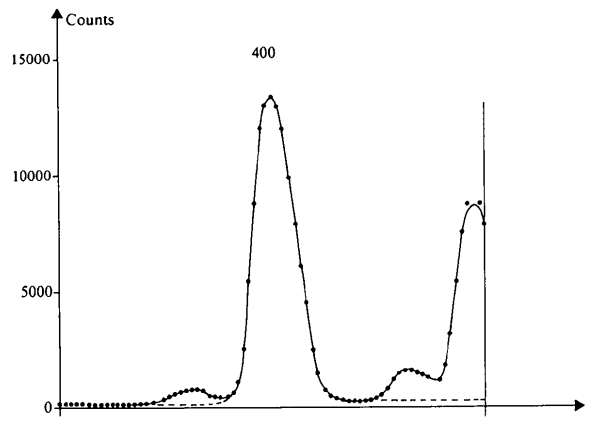

Fig. 1. An example of the step-scan of a reflection with contributions from several domains (full lines; 400 reflection). After corrections, spurious contributions are suppressed (broken line) and the corresponding counting values are introduced for the calculation of the integrated intensity.

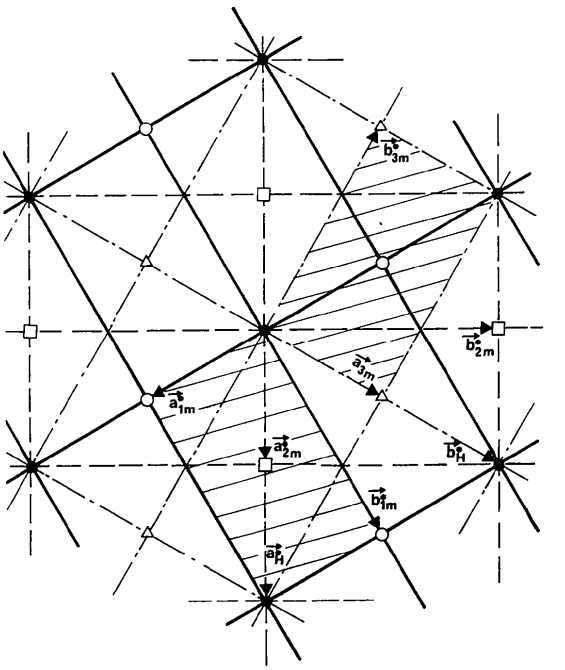

Fig. 2. Reciprocal-lattice phase perpendicular to $\mathbf{c}^*$ in the low-temperature phase. Full lines, broken lines and dot-dash lines represent, respectively, reciprocal lattices of the first, second and third domains. ●, fundamental peaks; ○, □, △, superlattice peaks of the first, second and third domains, respectively. The reciprocal cells of the first and third domains are hatched.

the calculated ones. This is due to the exact superposition of Bragg peaks of the selected domain and another domain. For these reflections, equivalent reflections $hh\bar{l}$ are measured and the corresponding intensities are introduced in the data collection. As a consequence, $00l$ reflections have been removed because of the non-existence of such equivalent reflections.

With these conditions, the R factor is 0·124 (wR = 0·146 with unit weights) (the y coordinate of the first C atom was fixed). Then, H atoms were geometrically placed on the benzene ring with a C—H bond length of 1·01 Å and a common isotropic temperature factor of 0·050 Å^2. Positional parameters and isotropic thermal parameters were again adjusted and the reliability R-factor fell to 0·107 (wR = 0·132). Anisotropic temperature factors were then introduced for C and O atoms, H atoms were again geometrically placed and their common isotropic temperature factor was also refined [U_H = 0·042(5) Å^2]. The final R factor is 0·066 (wR = 0·079, S = 1·64, unit weights). The 1893 reflections correspond to 1164 fundamental reflections ($h+k$ even) and 729 superlattice reflections ($h+k$ odd). The choice of a common temperature factor and geometrically determined positions for H atoms was influenced by the large number of parameters (433) with respect to the number of reflections with significant measured intensities. The maximum residual electronic density was ±0·40 e Å^{-3}.

The refinement may appear of poor quality, but at the end of the refinement some fundamental reflections remained where the intensity corrections of the non-selected domains were not correctly made. This is confirmed by a variance study: the mean deviation between calculated and measured structure factors for these fundamental reflections is twice that for the superlattice reflections where no spurious peaks appear.

Discussion

The final atomic coordinates are reported in Table 1 for T = 294 and 100 K and in Table 3 for T = 70 K.

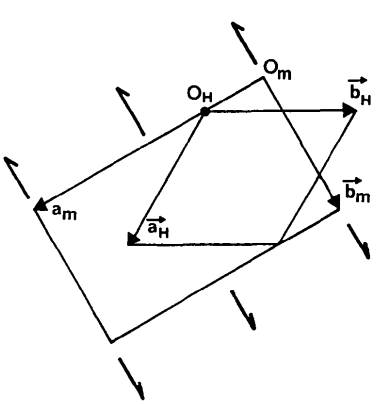

Fig. 3. The unit cell of the high- and low-temperature phases. The twofold screw axes common to the two phases are shown.

Table 1. *Positional parameters* (×10^4) *and equivalent isotropic Debye–Waller factors* (Å^2×10^3) *for benzil*

$U_{eq} = \frac{1}{3}$ trace (U).

	x	y	z	U_{eq}
T = 294 K				
C(0)	2262 (6)	1892 (7)	521 (3)	88 (7)
C(1)	2308 (6)	233 (6)	756 (3)	86 (6)
C(2)	2845 (7)	−2 (8)	1695 (4)	105 (8)
C(3)	2862 (8)	−1570 (9)	1932 (5)	152 (10)
C(4)	2346 (10)	−2942 (9)	1242 (6)	173 (12)
C(5)	1778 (8)	−2770 (8)	315 (5)	141 (10)
C(6)	1785 (7)	−1155 (7)	67 (4)	99 (8)
O	2577 (6)	3094 (5)	1114 (2)	132 (7)
T = 100 K				
C(0)	2305 (6)	1970 (6)	542 (3)	42 (5)
C(1)	2355 (5)	283 (5)	785 (3)	38 (4)
C(2)	2884 (6)	42 (7)	1743 (3)	49 (5)
C(3)	2903 (7)	−1549 (7)	1992 (4)	78 (7)
C(4)	2357 (7)	−2938 (7)	1284 (4)	80 (7)
C(5)	1814 (7)	−2738 (7)	335 (4)	63 (6)
C(6)	1832 (6)	−1132 (6)	84 (3)	43 (5)
O	2624 (5)	3181 (4)	1147 (2)	60 (4)

Table 2. *Bond lengths* (Å) *and bond angles* (°) *for benzil in the high-temperature phase*

C′(0) is generated from C(0) by the twofold molecular axis.

	T = 294 K	T = 100 K		T = 294 K	T = 100 K
C(0)–C(1)	1·449 (7)	1·467 (6)	C(2)–C(3)	1·363 (9)	1·379 (8)
C(0)–O	1·215 (6)	1·217 (5)	C(3)–C(4)	1·381 (10)	1·386 (7)
C(0)–C′(0)	1·523 (6)	1·529 (6)	C(4)–C(5)	1·385 (11)	1·386 (8)
C(1)–C(2)	1·407 (7)	1·403 (6)	C(5)–C(6)	1·396 (8)	1·376 (7)
C(1)–C(6)	1·387 (7)	1·397 (6)			
C(1)–C(0)–O	123·6 (5)	123·5 (4)	C(1)–C(2)–C(3)	120·8 (6)	121·1 (5)
C(1)–C(0)–C′(0)	120·6 (4)	118·8 (4)	C(2)–C(3)–C(4)	119·6 (7)	119·0 (5)
O–C(0)–C′(0)	115·8 (5)	117·6 (4)	C(3)–C(4)–C(5)	121·1 (7)	121·0 (5)
C(0)–C(1)–C(2)	120·1 (5)	120·2 (4)	C(4)–C(5)–C(6)	119·3 (6)	119·8 (5)
C(0)–C(1)–C(6)	120·6 (5)	121·2 (4)	C(1)–C(6)–C(5)	119·9 (5)	120·5 (4)
C(2)–C(1)–C(6)	119·2 (5)	118·6 (4)			

Bond lengths and bond angles are given in Table 2 for T = 294 and 100 K and in Table 4 for T = 70 K. An *ORTEP*II drawing (Johnson, 1976) of the contents of the unit cell of benzil at T = 294 K is given in Fig. 4.

Results at room temperature agree well with those of Brown & Sadanaga (1965). For the two studied temperatures of the high-temperature phase, high values of thermal coefficients are observed, particularly for atoms at the end of the benzene rings. At 70 K, a large decrease in these thermal coefficients was noticed. Attempts were made to express these thermal coefficients in terms of rigid-body-analysis coefficients (Schomaker & Trueblood, 1968) but the results were not decisive. This can be explained simply by the possibility of quasi-independent vibrations by each of the two parts of each molecule. Nevertheless, such calculations have been performed for a half molecule with the thermal coefficients of the high-temperature phase. There are large translational thermal vibrations along the threefold axis: 0·090 Å^2 at room temperature and 0·044 Å^2 at 100 K. Important rotational thermal vibrations are also observed around a direction approximately corresponding to the benzene-ring axis, their values are 58·5°^{2} at room temperature and 26·6°^{2} at 100 K.

Table 3. *Positional parameters* ($\times 10^4$) *and equivalent isotropic Debye-Waller factors* ($Å^2 \times 10^3$) *for benzil in the low-temperature phase* ($T = 70$ K)

$U_{eq} = \frac{1}{3}$ trace (U).

	x	y	z	U_{eq}
C(00)	2647 (6)	2015	449 (9)	24 (11)
C(01)	3494 (7)	1111 (11)	700 (7)	21 (11)
C(02)	3862 (7)	1246 (11)	1672 (7)	21 (11)
C(03)	4654 (7)	378 (12)	1877 (8)	29 (12)
C(04)	5080 (7)	−608 (13)	1163 (9)	36 (13)
C(05)	4727 (7)	−690 (13)	180 (9)	39 (13)
C(06)	3926 (6)	156 (11)	−57 (8)	27 (11)
C(10)	2307 (7)	2057 (11)	−643 (8)	29 (11)
C(11)	1404 (7)	1315 (11)	−866 (7)	21 (10)
C(12)	1039 (7)	1578 (12)	−1816 (7)	27 (11)
C(13)	201 (7)	868 (13)	−2063 (7)	27 (11)
C(14)	−249 (7)	−134 (13)	−1371 (9)	28 (13)
C(15)	114 (7)	−387 (11)	−426 (8)	30 (11)
C(16)	948 (7)	314 (11)	−175 (7)	27 (10)
C(20)	1379 (6)	−589 (11)	3892 (7)	20 (10)
C(21)	1336 (7)	1126 (11)	4153 (7)	22 (10)
C(22)	1061 (7)	1617 (12)	5137 (7)	31 (11)
C(23)	1048 (8)	3238 (13)	5361 (8)	30 (13)
C(24)	1308 (7)	4355 (11)	4657 (8)	28 (11)
C(25)	1585 (7)	3895 (12)	3698 (7)	26 (12)
C(26)	1594 (6)	2276 (11)	3440 (8)	27 (11)
C(30)	1542 (7)	−1104 (12)	2807 (7)	24 (10)
C(31)	2352 (6)	−2105 (11)	2554 (7)	22 (10)
C(32)	2439 (7)	−2771 (11)	1604 (7)	24 (11)
C(33)	3201 (8)	−3704 (11)	1357 (8)	38 (12)
C(34)	3879 (6)	−3980 (10)	2060 (7)	31 (11)
C(35)	3816 (7)	−3322 (12)	3029 (7)	35 (11)
C(36)	3037 (6)	−2378 (11)	3271 (7)	23 (10)
C(40)	3588 (6)	−1534 (11)	−2835 (8)	23 (11)
C(41)	2710 (6)	−2331 (11)	−2542 (7)	17 (9)
C(42)	2633 (6)	−2998 (11)	−1606 (8)	25 (11)
C(43)	1787 (7)	−3722 (12)	−1291 (8)	28 (12)
C(44)	1043 (7)	−3775 (12)	−1952 (9)	35 (13)
C(45)	1137 (7)	−3097 (13)	−2904 (8)	29 (12)
C(46)	1959 (7)	−2381 (12)	−3196 (8)	27 (12)
C(50)	3723 (6)	−998 (11)	−3925 (7)	19 (10)
C(51)	3715 (6)	732 (11)	−4166 (7)	19 (10)
C(52)	3942 (6)	1221 (12)	−5135 (7)	17 (10)
C(53)	3923 (7)	2836 (13)	−5380 (8)	28 (12)
C(54)	3670 (7)	3958 (11)	−4637 (9)	26 (12)
C(55)	3438 (7)	3460 (11)	−3671 (8)	26 (11)
C(56)	3488 (7)	1824 (11)	−3443 (6)	17 (10)
O(0)	2200 (5)	2786 (9)	1074 (6)	35 (9)
O(1)	2775 (5)	2811 (8)	−1233 (5)	31 (8)
O(2)	1229 (5)	−1642 (8)	4508 (5)	31 (8)
O(3)	968 (5)	−720 (8)	2187 (5)	28 (8)
O(4)	4241 (4)	−1350 (7)	−2291 (5)	27 (7)
O(5)	3862 (5)	−2058 (8)	−4558 (5)	29 (8)

Table 4. *Bond lengths* (Å) *and bond angles* (°) *for benzil in the low-temperature phase* ($T = 70$ K)

C(00)–C(01)	1·477 (12)	C(30)–C(31)	1·469 (13)
C(00)–C(10)	1·549 (16)	C(30)–O(3)	1·224 (12)
C(00)–O(0)	1·227 (12)	C(31)–C(32)	1·390 (13)
C(01)–C(02)	1·416 (13)	C(31)–C(36)	1·408 (13)
C(01)–C(06)	1·423 (14)	C(32)–C(33)	1·381 (15)
C(02)–C(03)	1·383 (14)	C(33)–C(34)	1·388 (14)
C(03)–C(04)	1·394 (15)	C(34)–C(35)	1·408 (13)
C(04)–C(05)	1·420 (17)	C(35)–C(36)	1·403 (13)
C(05)–C(06)	1·395 (14)	C(40)–C(41)	1·474 (13)
C(10)–C(11)	1·475 (14)	C(40)–C(50)	1·532 (14)
C(10)–O(1)	1·204 (12)	C(40)–O(4)	1·209 (11)
C(11)–C(12)	1·401 (13)	C(41)–C(42)	1·373 (14)
C(11)–C(16)	1·400 (13)	C(41)–C(46)	1·402 (14)
C(12)–C(13)	1·390 (14)	C(42)–C(43)	1·415 (14)
C(13)–C(14)	1·398 (15)	C(43)–C(44)	1·403 (15)
C(14)–C(15)	1·392 (16)	C(44)–C(45)	1·397 (16)
C(15)–C(16)	1·383 (14)	C(45)–C(46)	1·375 (14)
C(20)–C(21)	1·479 (13)	C(50)–C(51)	1·484 (13)
C(20)–C(30)	1·526 (13)	C(50)–O(5)	1·240 (11)
C(20)–O(2)	1·222 (11)	C(51)–C(52)	1·390 (13)
C(21)–C(22)	1·425 (13)	C(51)–C(56)	1·365 (13)
C(21)–C(26)	1·399 (14)	C(52)–C(53)	1·392 (15)
C(22)–C(23)	1·390 (15)	C(53)–C(54)	1·408 (15)
C(23)–C(24)	1·374 (15)	C(54)–C(55)	1·391 (16)
C(24)–C(25)	1·388 (14)	C(55)–C(56)	1·406 (13)
C(25)–C(26)	1·398 (14)		
C(01)–C(00)–C(10)	120·2 (8)	C(20)–C(30)–C(31)	119·0 (8)
C(01)–C(00)–O(0)	122·5 (8)	C(20)–C(30)–O(3)	118·4 (9)
C(10)–C(00)–O(0)	117·3 (8)	C(31)–C(30)–O(3)	122·5 (9)
C(00)–C(01)–C(02)	119·5 (8)	C(30)–C(31)–C(32)	119·7 (8)
C(00)–C(01)–C(06)	118·4 (8)	C(30)–C(31)–C(36)	119·9 (8)
C(02)–C(01)–C(06)	122·0 (9)	C(32)–C(31)–C(36)	120·4 (8)
C(01)–C(02)–C(03)	117·7 (9)	C(31)–C(32)–C(33)	120·1 (9)
C(02)–C(03)–C(04)	121·9 (10)	C(32)–C(33)–C(34)	119·9 (9)
C(03)–C(04)–C(05)	120·1 (10)	C(33)–C(34)–C(35)	121·6 (9)
C(04)–C(05)–C(06)	119·9 (10)	C(34)–C(35)–C(36)	118·0 (9)
C(01)–C(06)–C(05)	118·4 (9)	C(31)–C(36)–C(35)	120·1 (8)
C(00)–C(10)–C(11)	118·5 (8)	C(41)–C(40)–C(50)	118·4 (8)
C(00)–C(10)–O(1)	116·4 (9)	C(41)–C(40)–O(4)	124·8 (9)
C(11)–C(10)–O(1)	124·8 (9)	C(50)–C(40)–O(4)	116·7 (8)
C(10)–C(11)–C(12)	117·7 (9)	C(40)–C(41)–C(42)	118·5 (8)
C(10)–C(11)–C(16)	121·5 (9)	C(40)–C(41)–C(46)	121·0 (8)
C(12)–C(11)–C(16)	120·8 (9)	C(42)–C(41)–C(46)	120·5 (9)
C(11)–C(12)–C(13)	119·4 (9)	C(41)–C(42)–C(43)	119·9 (9)
C(12)–C(13)–C(14)	119·4 (9)	C(42)–C(43)–C(44)	119·2 (9)
C(13)–C(14)–C(15)	121·0 (10)	C(43)–C(44)–C(45)	120·0 (10)
C(14)–C(15)–C(16)	119·9 (9)	C(44)–C(45)–C(46)	120·1 (10)
C(11)–C(16)–C(15)	119·5 (9)	C(41)–C(46)–C(45)	120·3 (9)
C(21)–C(20)–C(30)	120·2 (8)	C(40)–C(50)–C(51)	119·4 (8)
C(21)–C(20)–O(2)	122·4 (8)	C(40)–C(50)–O(5)	117·1 (8)
C(30)–C(20)–O(2)	117·2 (8)	C(51)–C(50)–O(5)	123·5 (8)
C(20)–C(21)–C(22)	120·5 (8)	C(50)–C(51)–C(52)	119·2 (8)
C(20)–C(21)–C(26)	119·9 (8)	C(50)–C(51)–C(56)	120·2 (8)
C(22)–C(21)–C(26)	119·6 (9)	C(52)–C(51)–C(56)	120·6 (9)
C(21)–C(22)–C(23)	118·9 (9)	C(51)–C(52)–C(53)	120·0 (9)
C(22)–C(23)–C(24)	121·0 (10)	C(52)–C(53)–C(54)	119·2 (9)
C(23)–C(24)–C(25)	120·8 (9)	C(53)–C(54)–C(55)	120·5 (10)
C(24)–C(25)–C(26)	119·9 (9)	C(54)–C(55)–C(56)	118·8 (9)
C(21)–C(26)–C(25)	119·9 (9)	C(51)–C(56)–C(55)	120·8 (9)

To characterize the molecule deformations when the crystal crosses the transition, angles between the two equivalent parts of the molecule are calculated. These are the angles between the normals of the mean planes of the two benzene rings and the angle between the two C(i1)–C(i4) lines of the molecule, these being the mean directions of the benzene rings. The results of the calculations are reported in Table 5. No significant deformation of the molecule is observed between the two studied temperatures of the high-temperature phase. For the low-temperature phase, one of the three independent molecules is not distorted with respect to the high-temperature phase. For the two others, there are shifts of the order of ±5° for the two angles. So, large deformations of the molecules appear when the transition is crossed. Fig. 5 shows *ORTEP*II (Johnson, 1976) drawings in the two phases projected along the $\mathbf{c}^*$ axis (common to the two phases). The three molecules of the primitive unit cell of the low-temperature phase are presented with the corresponding ones of the high-temperature phase. The loss of the screw threefold axis is easily seen.

In this study, the space group of the low-temperature phase of benzil is assumed to be $P2_1$ with a twofold unit-cell expansion. But some experimental results have been explained in the framework of a fourfold unit-cell expansion, with space group $C2$. In particular, this is the case for the Raman scattering study of Moore *et al.* (1983). The fourfold unit-cell expansion, corresponding to 12 molecules per unit cell, leads to 69 external modes, all Raman active, 33 having the A symmetry and 36 the B symmetry. With a twofold unit-cell expansion (with six molecules per unit cell), there are 33 external modes

Table 5. *Characteristic angles* (°) *between the two parts of the molecule of benzil*

	Room temperature	$T = 100$ K	$T = 70$ K Molecule 1 $i = 0, i' = 1$	Molecule 2 $i = 2, i' = 3$	Molecule 3 $i = 4, i' = 5$
Angles between normals of benzene rings	103·2	102·9	103·1	108·7	98·3
Angles C(i1)–C(i4)/C(i'1)–C(i'4)	123·0	122·0	122·6	128·0	117·9

with 15 in the A symmetry and 18 in the B symmetry. The authors, quoted above, find experimentally at low temperature 17 A modes and 19 B modes which agree with a fourfold expansion of the unit cell. In fact, with the existence of domains, polarization directions change with them. If, for a selected domain, the polarization state is $(XY+XZ)$ to obtain only B modes, for the two other domains, there are components where A modes are active. The existence of domains leads to the simultaneous existence of A and B modes in this polarization state. From the Raman results of Moore *et al.* (1983), this fact is confirmed by the near frequency values and the same temperature dependence of modes obtained with the $(XY+XZ)$ and (ZZ) polarization states. For the (ZZ) polarization, the high-temperature-phase ($T =$ 173 K) E modes, normally inactive, appear. The corresponding modes must also appear in the low-temperature phase. Taking into account all these reasons, we find that the number of the true modes with A and B symmetries can be lower than 15 and 18 and so can correspond to a twofold unit-cell expansion.

In the light of these new structural results, a model of the mechanism of the transition is in progress.

The authors thank F. Baert, R. Fouret and P. Zielinski for helpful discussions. The building of the four-circle spectrometer was supported by a grant from ANVAR.

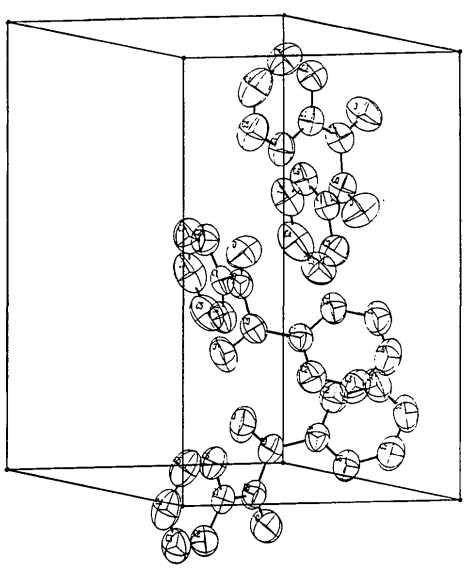

Fig. 4. The unit-cell contents of benzil in the high-temperature phase at room temperature.

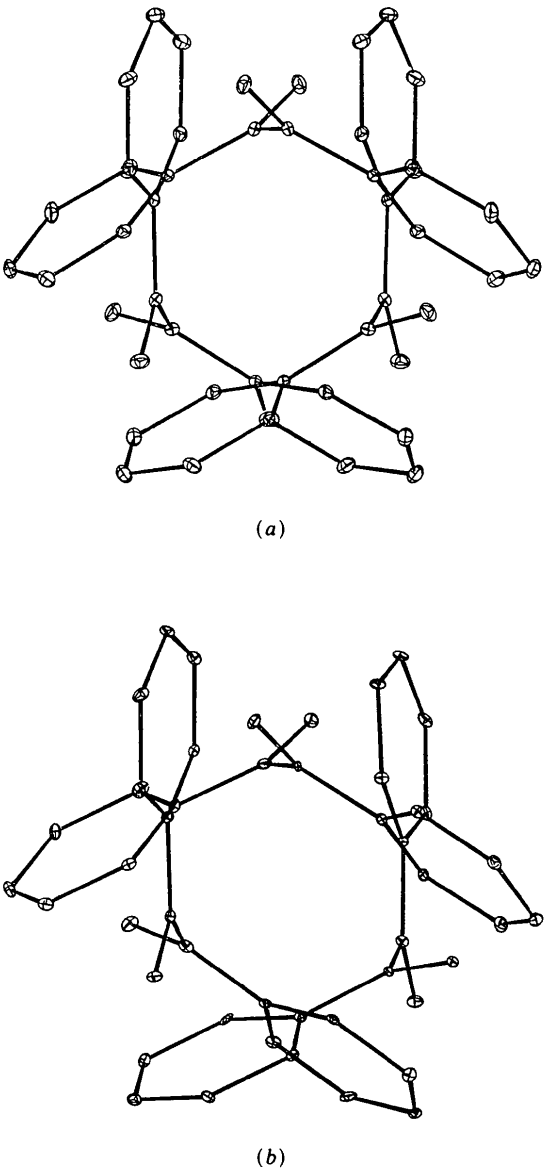

Fig. 5. *ORTEP*II projections along the c^* axis (*a*) at 100 K, in the high-temperature phase; (*b*) at 70 K, in the low-temperature phase.

References

AUBRY, S. & PICK, R. (1971). *J. Phys. (Paris)*, **32**, 657-670.
BROWN, C. J. & SADANAGA, R. (1965). *Acta Cryst.* **18**, 158-164.
CHAN, Y. L. & HEATH, B. A. (1979). *Mol. Cryst. Liq. Cryst.* **52**, 45-52.
DWORKIN, A. & FUCHS, A. H. (1977). *J. Chem. Phys.* **67**, 1789-1790.
ESHERICK, P. & KOHLER, B. E. (1973). *J. Chem. Phys.* **59**, 6681-6682.
HIGASHI, K. (1938). *Bull. Chem. Soc. Jpn*, **13**, 158-159.
International Tables for X-ray Crystallography (1974). Vol. IV. Birmingham: Kynoch Press. (Present distributor D. Reidel, Dordrecht).
JOHNSON, C. K. (1976). *ORTEP*II. Report ORNL-5138, Oak Ridge National Laboratory, Tennessee, USA.
MOORE, D. R., TEKIPPE, V. J., RAMDAS, A. K. & TOLEDANO, J. C. (1983). *Phys. Rev.* B**27**, 7676-7690.
ODOU, G. (1976). Thesis, Univ. of Lille, France. (Unpublished.)
ODOU, G., MORE, M. & WARIN, V. (1978). *Acta Cryst.* A**34**, 459-462.
SAMSON, S., GOLDISH, E. & DICK, C. J. (1980). *J. Appl. Cryst.* **13**, 425-432.
SAPRIEL, J., BOUDOU, A. & PERIGAUD, A. (1979). *Phys. Rev. B*, **19**, 1484-1491.
SCHOMAKER, V. & TRUEBLOOD, K. N. (1968). *Acta Cryst.* B**27**, 63-76.
SHELDRICK, G. M. (1976). *SHELX*76. Program for crystal structure determination. Univ. of Cambridge, England.
SOLIN, S. A. & RAMDAS, A. K. (1968). *Phys. Rev.* **174**, 1069-1075.
TERAUCHI, H., KOJIMA, T., SAKAUE, K., TAJIRI, F. & MAEDA, H. (1982). *J. Chem. Phys.* **76**, 612-615.
TOLEDANO, J. C. (1979). *Phys. Rev. B*, **20**, 1147-1156.
VACHER, R., BOISSIER, M. & SAPRIEL, J. (1981). *Phys. Rev. B*, **23**, 215-220.
WYNCKE, B., BREHAT, F. & HADNI, A. (1980). *Ferroelectrics*, **25**, 617-620.
YOSHIHARA, A., BERNSTEIN, E. R. & RAICH, J. C. (1982). *J. Chem. Phys.* **77**, 2768-2778.
YOSHIHARA, A., BERNSTEIN, E. R. & RAICH, J. C. (1983). *J. Chem. Phys.* **79**, 2504-2514.
YOSHIHARA, A., WILBER, W. D., BERNSTEIN, E. R. & RAICH, J. C. (1982). *J. Chem. Phys.* **76**, 2064-2072.

SHORT COMMUNICATIONS

Contributions intended for publication under this heading should be expressly so marked; they should not exceed about 1000 *words; they should be forwarded in the usual way to the appropriate Co-editor; they will be published as speedily as possible.*

Acta Cryst. (1987). B**43**, 405-406

An alternative approach to a revision of van der Waals radii for molecular crystals.

By D. KIRIN, *Rudjer Bošković Institute, POB* 1016, 41001 *Zagreb, Yugoslavia*

(*Received* 4 *November* 1986; *accepted* 28 *January* 1987)

Abstract

Recently Nyburg & Faerman [*Acta Cryst.* (1985), B**41**, 274-279] made a revision of non-bonding (van der Waals) radii of atoms in molecular crystals. It was shown that the effective shape of atoms in crystals is spheroidal (elliptical) with two radii, major r_a and minor r_b. In the present paper an alternative approach to the interpretation of their data is proposed. As a result, atoms in crystals still have spherical shape but the centre of the sphere is displaced from the nuclear site along the chemical bond. The implications of the model for the formulation of empirical atom-atom intermolecular potentials are briefly discussed.

Recently Nyburg & Faerman (1985; henceforth NF) published an extensive study of the non-bonded contacts in molecular crystals with N, O, F, S, Se, Cl, Br and I atoms attached to a carbon atom. The study, based on the Cambridge Structural Database, enabled them to conclude that the effective shape of atoms (as described by the van der Waals radius) in molecular crystals is not spherical but spheroidal (elliptical), with shorter radius along the atom-to-carbon vector ('polar flattening').

This conclusion was derived from the analysis of a large number of intermolecular distances d_{XX} (X being one of the previously mentioned atoms). The analysis of the contact scatterplots (polar diagram of d_{XX} distances *versus* angle μ between d_{XX} and the C–X bond) led to the definition of a boundary for the region where there are intermolecular contacts (Fig. 1 in NF). The authors concluded that this boundary is generally ellipsoidal with two radii, major r_a and minor r_b. The exact placing of the boundary was subjective and was not obtained from some fitting procedure. Thus, while some atoms are spherical (N and O) with both radii equal, some others are spheroidal with a significant difference between the two radii r_a and r_b (Table 1 in NF).

The purpose of the present note is to propose an alternative model for the description of the data presented by NF. The boundary line could equally well be a *circle*, whose centre is displaced from the atom position along the C–X bond toward the carbon atom. The value of the shift, Δ, is related to the difference between the NF major and minor radii, r_a and r_b. The proposed model is illustrated in Fig. 1 where the data for iodine are plotted (taken from NF). The full line is the NF ellipse with major radius $2r_a = 4{\cdot}26$ Å and minor radius $2r_b = 3{\cdot}52$ Å. The dashed circle is our proposed boundary with $R = 2r_a$. In order to get a satisfactory agreement with the scatterplot, the centre was shifted by 0·6 Å from the origin. It can be seen that such a boundary fits the data equally well. A similar analysis could be performed for other atoms (Cl, Br, S, Se).

0108-7681/87/040405-02$01.50